



Key features

- **Dynamic Growth Insights:** Monitor the spike number and its distribution changes over time to reflect growth dynamics accurately.
- **Automated Spike Analysis:** Utilize the Spike APP module within the PlantScreen™ SW toolbox for automated spike number analysis.
- **Genetic Diversity Insights:** Gain insights into the genetic diversity influencing heading time and floral development, critical agronomic traits.
- **Cultivar Performance Evaluation:** Investigate how different cultivars with varying yield potentials perform under various stress conditions and environmental factors.

The spike is a critical yield organ in both wheat (*Triticum aestivum*) and barley (*Hordeum vulgare*). Measuring spike number per unit area and extracting morphological features are essential for yield estimation, plant health assessment, and guiding breeding decisions. High-throughput, image-based analysis for **non-invasive spike assessment**, including determining **heading time** and **yield-related traits**, is highly desirable in automated phenotyping. However, accurately detecting grain spikes is complex due to their small image area and similarity in color to surrounding plant leaves, posing challenges even for advanced deep neural networks (DNNs).

Spike APP is a new tool applying latest computer vision methodology for image-based analysis of spikes and rapid determination of flowering time-related growth stages in wheat and barley. Leveraging the advanced capabilities of attention mechanism-based deep learning models, **Spike APP** accurately detects small and subtle features of grain spikes. The Spike APP employs advanced pre-trained Yolov4 and Yolov8x models to achieve high precision in the automated detection, segmentation, and phenotyping of spikes in greenhouse-grown barley and wheat. It targets both inner and top spikes with an average precision for spike prediction (AP0.5) of 0.79. The Spike APP is configured to communicate with the PlantScreen™ Data Analyzer through a dedicated database setup to facilitate seamless data exchange and processing including spike localization, extraction of essential phenotypes and the generation of Region of Interest (ROI) boxes.

Key extracted traits

- Spike detection and counting
- Identification of growth stages associated with heading time
- Spike development during late reproductive and grain-filling phases
- Single spike morphological analysis including spike area

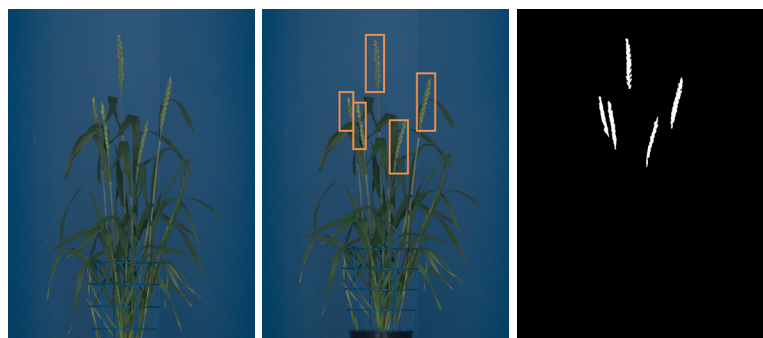


Fig.1 Example of spike detection and segmentation of barley images: (a) RGB mage of a mature plant, (b) detection of spikes by ROI boxes, (c) pixel-wise segmentation of spikes.

Methodology

YOLOv4 and YOLOv8x are trained on datasets of varying sizes and utilized for spike detection in both barley and wheat. The hyperparameters are configured as follows: 1000 epochs, a batch size of 32, an initial learning rate of 0.01, momentum set at 0.93, and a weight attenuation coefficient of 0.0005. The trained model's performance is evaluated using both validation and test sets (Fig.2, 3).

| Training set | Test set | |
|----------------------|--------------|--|
| 810 | 200 | |
| Spike Detection DNNs | Backbone | Average precision (AP _{0.5}) |
| Yolov4 | CSPDarknet53 | 0.78 |
| Yolov8x | CSP Dark Net | 0.79 |

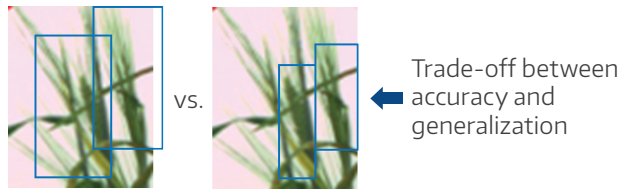


Fig.2 Ground truth consideration for training set. Ground truth data were generated to include localized ROI around the spike and also the spike awn.

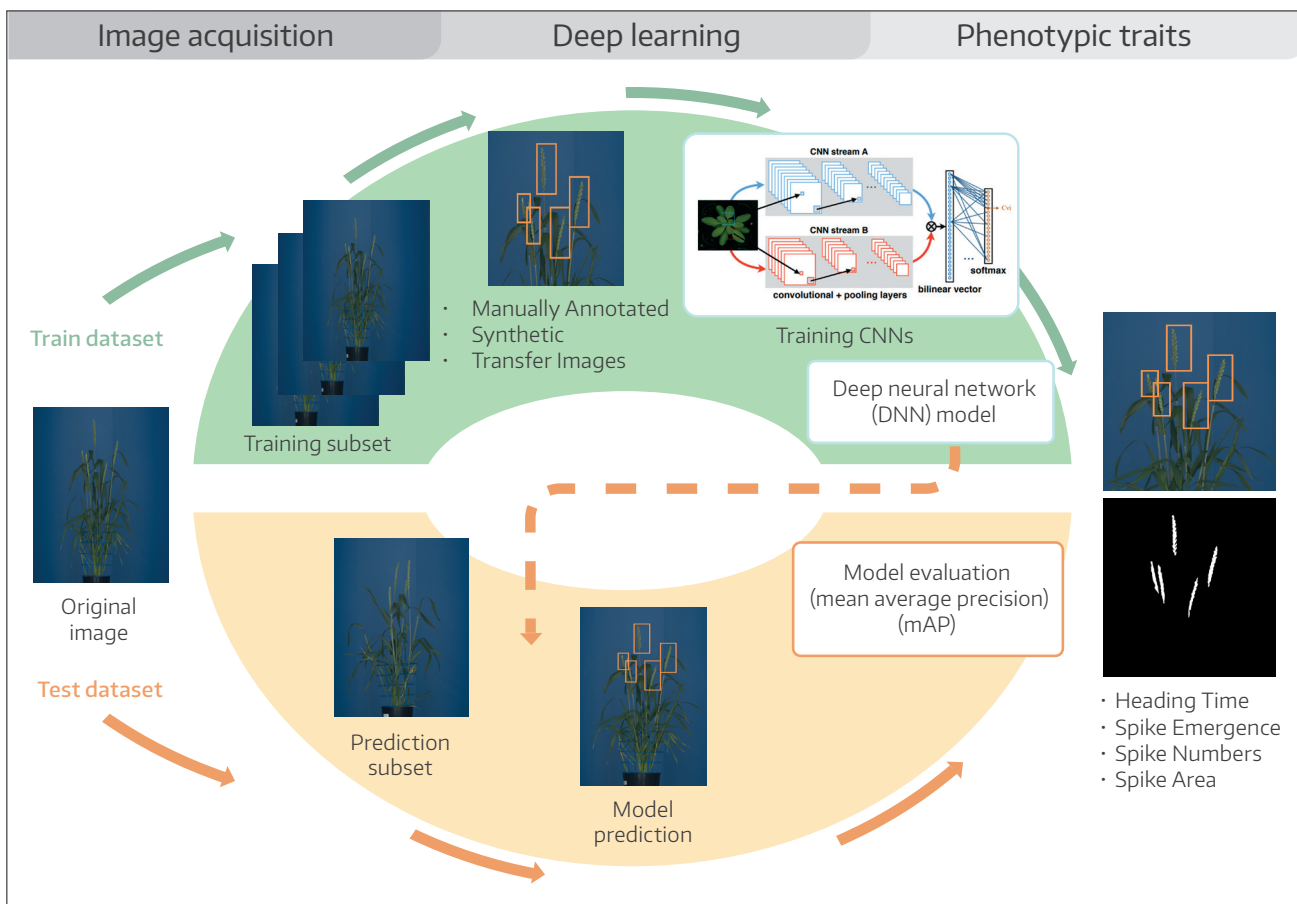


Fig 3. Overall scheme of supervised spike detection.

Case study

In this study, nine spring barley (*Hordeum vulgare L*) genotypes with diverse genetic backgrounds were selected to examine the impact of drought stress on their morphological and physiological responses throughout their developmental stages. During the reproductive phase, assessments were made on the **heading time** (when spikes begin to emerge) and the **development rate** of spikes.

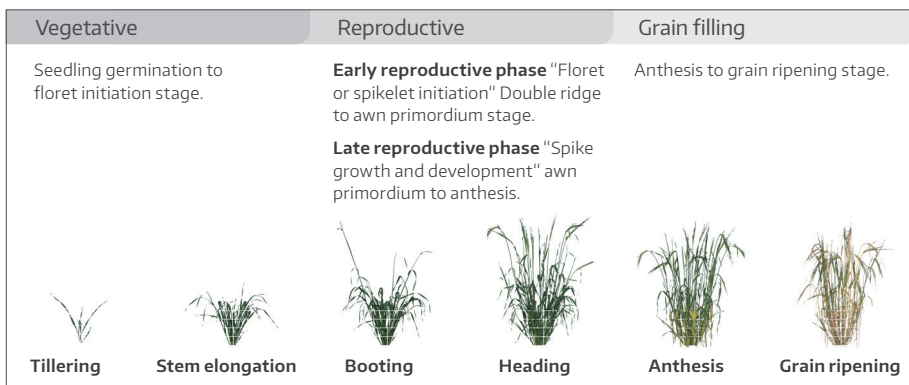
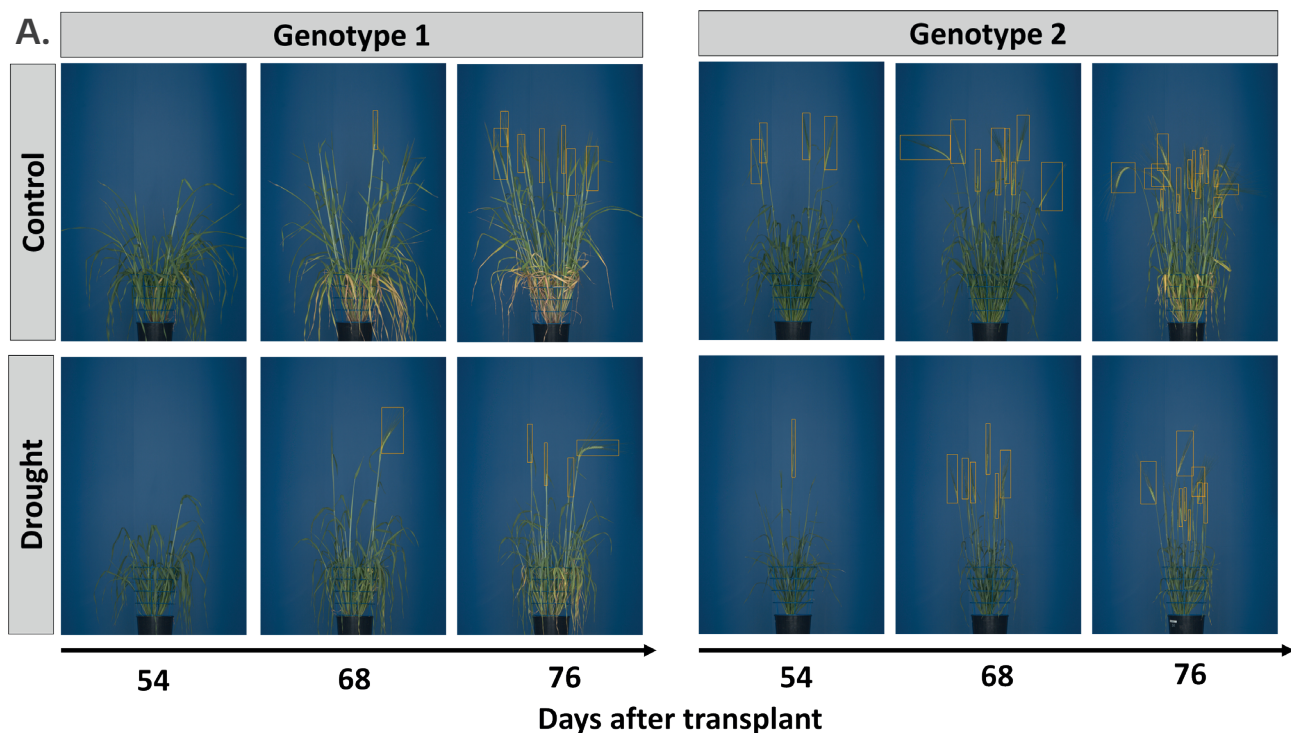


Fig 4. Major developmental stages in barley.



Case study validation

Hundreds of RGB images from PlantScreen™ high-throughput phenotyping system were analyzed to extract morphological traits related to spike development. Figure 4 provides an overview of the key development phases in barley and wheat. We monitored spike development from the initiation of the heading stage (late reproductive stage, Zadoks 51) to the grain ripening stage (Zadoks 91).

Figure 5 illustrates the differences in spike development between two genotypes (early and late heading time) under control and drought conditions over period of six weeks.

We show high linear correlation between virtual spike number count and the ground truth manual count of spike number among the nine genotypes ($R^2 = 0.74$) (Fig. 6). Among the nine genotypes we quantified significant phenotypic variation in spike number and heading time under both environments. Under drought conditions spike number was reduced in range of 30-50 %. Additionally, we investigated spike emergence (Zadoks 51) as a crucial transition in the reproductive phase (Fig.7) .

The high determination coefficient ($R^2 = 0.95$) between the image-based data sets as compared with the manual data shows that the model can robustly identify **spike emergence** and **heading time**.

The results from the **Spike App** tool, the integrated deep learning platform for spike detection, demonstrate its significant potential for enhancing the efficiency and reproducibility of spike analysis during the phenotyping of large populations (Fig.8).

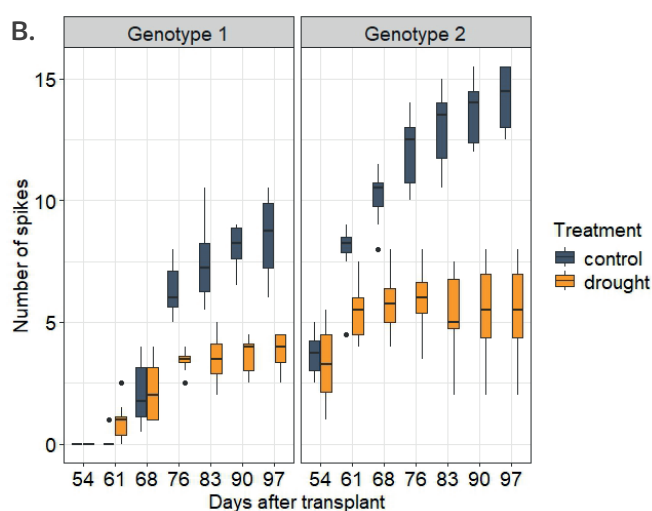


Figure 5. (A) RGB side view images in two barley genotypes under control and drought stress selected from three-time points. (B) Model-based counting of spike number during late reproductive stage till grain filling stage



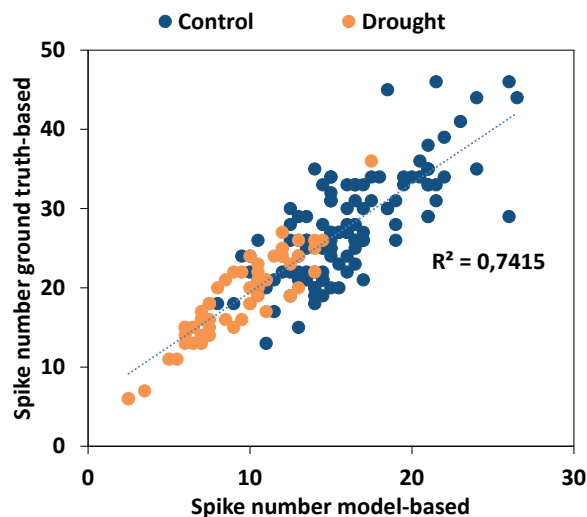


Figure 6. Correlation between virtual spike number count (RGB images acquired 87 days after transplantation) and the ground truth manual count of spike number (harvested 129 days after transplant).

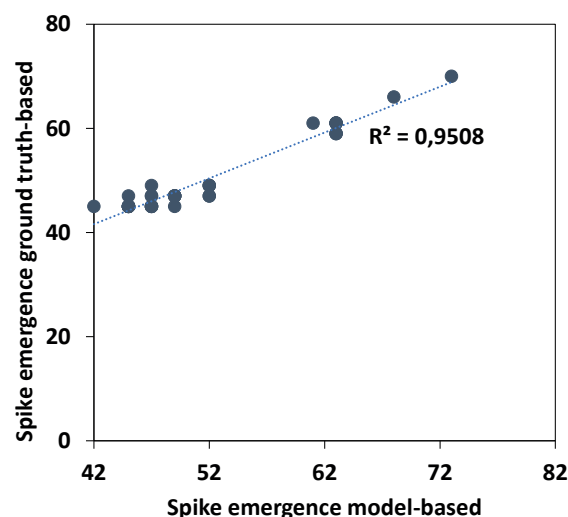


Figure 7. Correlation between spike emergence model- and ground truth-based data in early and late genotypes during the initiation of heading stage

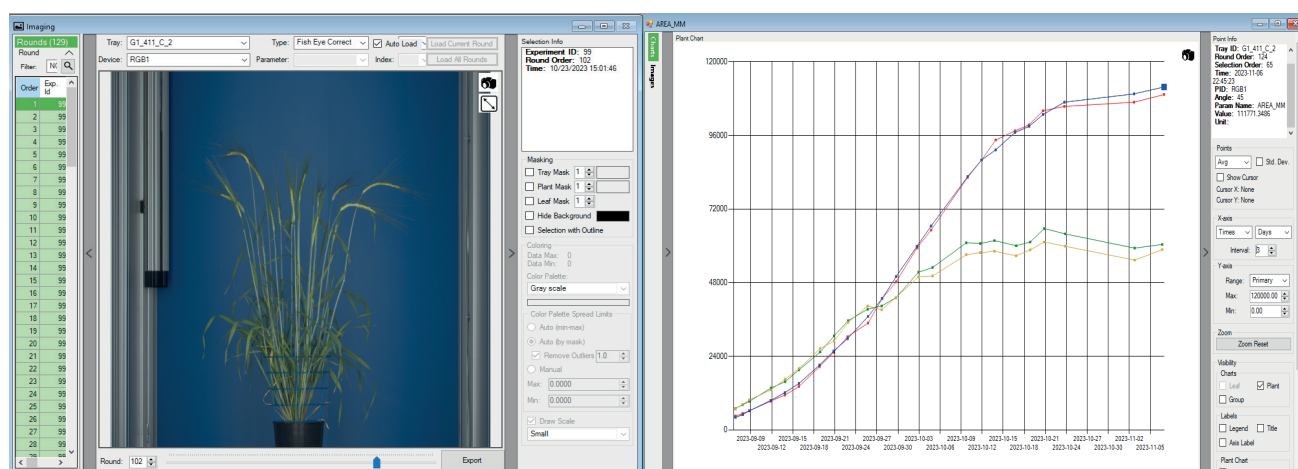


Figure 8. Visualisation of the extracted traits in PlantScreen™ Analyzer SW.

References:

Ullah S, Henke M, Narisetti N, Panzarová K, Trtílek M, Hejatkó J, Gladilin E. 2021.

<https://doi.org/10.3390/s21227441>

Ullah S., Panzarová K., Trtílek M., Lexa M., Máčala V., Neumann K., Altmann T., Hejatkó J., Pernisová M. and Gladilin E. 2024.

<https://spj.science.org/doi/10.34133/plantphenomics.0155>

Zadoks, J.C., Chang, T.T., Konzak, C.F. 1974.

<https://doi.org/10.1111/j.1365-3180.1974.tb01084.x>.

Narisetti N, Neumann K, Röder MS, Gladilin E. 2020.

<https://doi.org/10.3389/fpls.2020.00666>

Misra T, Arora A, Marwaha S, Chinnusamy V, Rao AR, Jain R, Sahoo RN, Ray M, Kumar S, Raju D, et al. 2020.

<https://doi.org/10.1186/s13007-020-00582-9>



PlantScreen™ Systems

Complete Solutions for Automated Phenotyping

Seeing beyond the surface

